Contemporary Mathematics
http://ojs.wiserpub.com/index.php/CM/

UNIVERSAL WISER PUBLISHER

Research Article

Analysis of Radial Distribution Systems Using Particle Swarm Optimization under Uncertain Conditions

M. Naveen Babu*, P. K. Dhal

Department of Electrical and Electronics Engineering, Vel Tech Rangarajan Dr. Sagunthala R&D Institute of Science and Technology, Chennai 600062, India
E-mail: naveenbabum76@gmail.com

Received: 1 August 2023; **Revised:** 14 August 2023; **Accepted:** 29 August 2023

Abstract: Efficiently mitigating losses in power distribution networks is imperative for their optimal operation. This research employs the particle swarm optimization (PSO) algorithm to investigate the joint optimization of phase balance and conductor sizing in imbalanced distribution systems. Objective functions encompass power loss, voltage unbalance, total neutral current, and complex power unbalance. Each objective is individually optimized before being integrated with weights to address multi-objective optimization. The study aims to minimize losses in inherently unequal electrical distribution networks. PSO techniques, namely power flow and optimal distributed generation (DG) placement, effectively curtail losses. These techniques are seamlessly integrated into existing systems using a tailored load-flow method for three-phase imbalanced radial distribution networks. Precise evaluation of network conditions relies on key metrics, including node voltage, angle, branch current, active and reactive power losses, and branch losses. A systematic approach identifies relevant variables, calculating target voltage angle and magnitude. Despite the time and effort required, this process yields accurate outcomes. A uniform voltage of 1 p.u. is maintained from substation to terminal node, with variable magnitude and phase angle adjustments yielding voltage drop computations. The proposed study is demonstrated on 19- and 25-node networks with unbalanced distribution. The results of the study underscore DG's potential for cost reduction and performance enhancement.

***Keywords*:** DG, radial distribution network, PSO, unbalanced system

MSC: 90C27, 90C31

Nomenclature

ACO	Ant colony optimization
BWO	Blue whale optimization
DG	Distributed generation
GA	Genetic algorithm
IAICA	Improved adaptive imperialist competitive algorithm
PSO	Particle swarm optimization
SCADA	Supervisory control and data acquisition

DOI: https://doi.org/10.37256/cm.6120253478

URDN Unbalanced radial distribution network
URDS Unbalanced radial distribution system

1. Introduction

Grid and off-grid modes are the two common practices for supplying electric power to the end-users. The power grid comprises three primary components: the power plant, transmission lines, and the distribution grid. Among these, the distribution system holds particular significance due to its responsibility for delivering electricity safely and cost-effectively to end users [1-4]. The distribution system is an integral component of a power grid, responsible for efficiently delivering electricity to end users. Reducing losses within this system is imperative for optimal operation [5-6]. However, the distribution network accounts for the majority of losses, attributed to low operating voltages and high R/X ratios.

An imbalance in a radial distribution system can refer to either an unbalance in load distribution or an imbalance in voltage levels among the different phases. Inherent imbalances in distribution networks result from unbalanced single-phase loads across the three-phase distribution system and non-equilateral conductor spacing. Consequently, voltage and current imbalances arise, along with increased overall neutral current triggering unnecessary relays and further decline the distribution system's service quality and reliability. To counter these challenges, proper phase balancing methods are imperative for unbalanced distribution systems, alongside the vital goal of minimizing power loss. While addressing phase imbalances is crucial, minimizing system power losses is equally essential. Distributing power to residences and businesses falls within the domain of the distribution system, a subset of the electrical grid [6]. Unequal distribution of single-phase or three-phase loads across different phases can result in imbalances. For example, if one phase has significantly higher loads than the others, it can lead to current and voltage imbalance, further, faults such as short circuits or ground faults in the network can cause imbalances. A comprehensive understanding of creating the phase impedance matrix is discussed in [7-9].

It's evident that unbalanced branch currents cause voltage imbalance among phases. Since power hinges on voltage and current, imbalances in either can lead to power loss and intricate power discrepancies. In view of these challenges in unbalanced distribution systems, planners are compelled to devise effective planning approaches. Distribution system planning ensures secure and reliable operations within defined parameters [10]. This encompasses designing new distribution networks/systems with modified wire configurations and phase loadings. Design challenges in unbalanced distribution systems include heightened losses, voltage imbalances, and power disparities. To ensure reliable operation, designing unbalanced distribution systems necessitates low power loss, balanced voltage, current, and power. Reconfiguration and optimization approaches can enhance system reliability by selecting appropriate tie switches. Modern optimization techniques, such as heuristic algorithms, mimic natural processes to formulate adaptable solutions applicable across various domains. In this study, we employ a hybrid optimization approach to enhance radial distribution network design while minimizing power losses. Miu et al. [11] proposed a fully simulated three-phase radial power-flow solution. Their method established the existence and uniqueness of a three-phase radial load-flow solution based on practical voltage levels and monotonous behavior. This method offers insights into enhancing distribution network management and planning. For asymmetric radial distribution systems, [12] introduced a load-flow technique using a matrix constructed through the Jacobian matrix process, avoiding laborious methodologies. Their approach adapts readily to distribution network paradigms and proves effective for substantial distribution settings.

In [13], a backward-forward load-flow method with neutral grounding was applied to a three-phase, four-wire radial distribution network, backed by test results on an imbalanced distribution network. In [14], the authors have proposed a power-flow technique for unbalanced distribution networks incorporating branch voltage mutual coupling, testing it on four unbalanced distribution networks. A method for analyzing power flows in imbalanced radial distribution systems, leveraging network analysis fundamentals and storing data as vectors, ensuring speed and accuracy applicable to various power-flow research domains is demonstrated in [15]. Utilizing the backward/forward sweep technique and the distribution transformer nodal admittance matrix, [16] devised an approach for imbalanced radial distribution networks, resolving phase shifts resulting from transformer winding connection switching. The authors of reference [17] have suggested a load-flow algorithm for balanced and unbalanced radial distribution systems based on the S-E power-flow algorithm, proving its efficiency across networks of various sizes. The reference [18] describes a load-flow method for imbalanced distribution networks, breaking down the solution into phases and in-phase components, effectively handling

complex distribution networks. A novel power-flow method for balanced and unbalanced radial distribution networks, solving equations for current injection using the Newton-Raphson method [19].

For the integration of load models, [20-21] introduced a load-flow approach based on fuzzy methodology, successfully applied to different-sized test systems. To enhance the voltage profile and reduce power losses, various algorithms [22-28] have been proposed in the literature for reconfiguration strategy by utilizing an IAICA, validated through simulation. The reference [29] suggests a network reconfiguration mechanism to balance feeder loads and prevent overloads, optimizing with Tabu search. The planning challenges of unbalanced distribution networks call for robust algorithms [30-33]. With the need to enhance the design of imbalanced distribution systems and the efficacy of metaheuristic algorithms, future exploration into statistical performance comparisons of various metaheuristics holds promise. These efforts are critical to effective planning and design, particularly in systems with DG integration.

2. Material and methodology

2.1 *Load-flow study of unbalanced radial distribution networks*

The study of a steady-state power system operating under specified parameters of power input, load demand, and network topology is performed with the help of a simple calculation called load-flow analysis. The load-flow process of any radial distribution network allows the determination of several parameters, including the magnitude and direction of voltage at each node, the active and reactive power supplied at the substation, the actual and reactive power flows in each line segment, and the losses in the system. Figure 1 illustrates a crucial element of the distribution network. Most of the stated load-flow work was conducted using a balanced distribution network as the basis. In this article, we demonstrate the load-flow approach for imbalanced networks that exist in the real world. The load-flow process of any radial distribution network can identify the amplitude and direction of voltage at each node, the active and reactive power supplied at the substation, the actual and reactive power flows in each line segment, and system losses. Figure 1 depicts a key distribution network component. The series impedance of the *n*th line and phase impedances are shown.

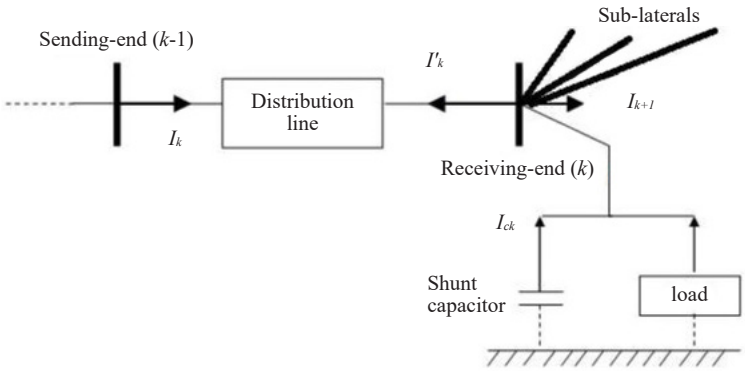

Figure 1. Basic block diagram of distribution system

$$Z_{An} = R_{An} + jX_{An}$$

$$Z_{Bn} = R_{Bn} + jX_{Bn}$$

$$Z_{Cn} = R_{Cn} + jX_{Cn} \quad (1)$$

The real power is P and reactive power is Q, which is related to complex power (S). The complex power for phases

A, B and C are indicated by Equation 2 [18, 28, 33]. Equation 3 indicates the branch current from bus k to bus $k + 1$ (branch-jj) and phases A, B, and C.

$$\begin{aligned}
\left(S_D\right)_{A(k)} &= \left(P_D\right)_{A(k)} + j\left(Q_D\right)_{A(k)} \\
\left(S_D\right)_{B(k)} &= \left(P_D\right)_{B(k)} + j\left(Q_D\right)_{B(k)} \\
\left(S_D\right)_{C(k)} &= \left(P_D\right)_{C(k)} + j\left(Q_D\right)_{C(k)}
\end{aligned} \tag{2}$$

$$\begin{aligned}
I_{A(j)} &= \frac{\left|V_{A(k)}\right|\angle\delta_{A(k)} - \left|V_{A(k+1)}\right|\angle\delta_{A(k+1)}}{Z_{A(j)}} \\
I_{B(j)} &= \frac{\left|V_{B(k)}\right|\angle\delta_{B(k)} - \left|V_{B(k+1)}\right|\angle\delta_{B(k+1)}}{Z_{B(j)}} \\
I_{C(jj)} &= \frac{\left|V_{C(k)}\right|\angle\delta_{C(k)} - \left|V_{C(k+1)}\right|\angle\delta_{C(k+1)}}{Z_{C(j)}}
\end{aligned} \tag{3}$$

where $\left|V_{A(k)}\right|\angle\delta_{A(k)}, \left|V_{B(k)}\right|\angle\delta_{B(k)}, \left|V_{C(k)}\right|\angle\delta_{C(k)}$ are the voltage magnitudes and phase angle of phase A, phase B and phase C at the kth node, $\left|V_{A(k+1)}\right|\angle\delta_{A(k+1)}, \left|V_{B(k+1)}\right|\angle\delta_{B(k+1)}, \left|V_{C(k+1)}\right|\angle\delta_{C(k+1)}$ are the voltage magnitude and phase angle of the phase A, phase B and phase C at $(k + 1)$th node.

Equation 4 represents phases A, B, and C branch currents.

$$\begin{aligned}
I_{A(jj)} &= \frac{P_{A(k+1)} - jQ_{A(k+1)}}{V^*_{A(k+1)}} \\
I_{B(jj)} &= \frac{P_{B(k+1)} - jQ_{B(k+1)}}{V^*_{B(k+1)}} \\
I_{C(jj)} &= \frac{P_{C(k+1)} - jQ_{C(k+1)}}{V^*_{C(k+1)}}
\end{aligned} \tag{4}$$

$P_{m(k+1)}$ and $Q_{m(k+1)}$ are the total real and reactive power load at the $(k + 1)$th node and are obtained by

$$P_{m(k+1)} = \sum_{j=k+1}^{n_{\text{bus}}} \left(P_D\right)_{m(j)} + \sum_{jj=jj+1}^{n_{\text{branch}}} \left(P_{\text{Loss}}\right)_{m(jj)}$$

$$Q_{m(k+1)} = \sum_{j=k+1}^{n_{\text{bus}}} \left(Q_D\right)_{m(j)} + \sum_{jj=jj+1}^{n_{\text{branch}}} \left(Q_{\text{Loss}}\right)_{m(jj)} \tag{5}$$

For end-node,

$$\left(P_m\right)_{n_{\text{bus}}} = \left(P_{D_m}\right)_{n_{\text{bus}}} \tag{6}$$

$$\frac{\left|V_{m(k)}\right| \angle \delta_{m(k)} - \left|V_{m(k+1)}\right| \angle \delta_{m(k+1)}}{Z_{m(j)}} = \frac{P_{m(k+1)} - jQ_{m(k+1)}}{V^*_{m(k+1)}} \tag{7}$$

$$\left|V_{m(k)}\right|^2 \left|V_{m(k+1)}\right|^2 = \left[\left|V_{m(k+1)}\right|^2 + \left(P_{m(k+1)}R_{m(jj)} + Q_{m(k+1)}X_{m(jj)}\right)\right]^2 + \left[P_{m(k+1)}X_{m(jj)} - Q_{m(k+1)}R_{m(jj)}\right]^2 \tag{8}$$

$$\left|V_{m(k+1)}\right|^4 + 2.0 \times \left[\left(P_{m(k+1)}R_{m(j)} + Q_{m(k+1)}X_{m(j)}\right) - \frac{\left|V_{m(k)}\right|^2}{2}\right] \times \left|V_{m(k+1)}\right|^2 + \left(R^2_{m(jj)} + X^2_{m(jj)}\right)\left(P^2_{m(k+1)} + Q^2_{m(k+1)}\right) = 0 \tag{9}$$

The voltage of each node of the phases *A*, *B* and *C* can be computed by above equations.

$$\left|V_{m(k+1)}\right| = \sqrt{\sqrt{\left[\left(P_{m(k+1)}R_{m(ij)} + Q_{m(k+1)}X_{m(ij)} - \frac{\left|V_{m(k)}\right|^2}{2}\right)^2 - \left(R^2_{m(ij)} + X^2_{m(ij)}\right)\left(P^2_{m(k+1)} + Q^2_{m(k+1)}\right)\right]} - \left(P_{m(k+1)}R_{m(ij)} + Q_{m(k+1)}X_{m(ij)} - \frac{\left|V_{m(k)}\right|^2}{2}\right)} \tag{10}$$

Equation (11) is used to calculate the angles of node voltage. Equations (12) and (13) yield the three-phase branch *jj* actual and reactive power losses.

$$\delta_{m(k)} - \delta_{m(k+1)} = \tan^{-1}\left[\frac{P_{m(k+1)}X_{m(jj)} - Q_{m(k+1)}R_{m(jj)}}{\left|V_{m(k+1)}\right|^2 + P_{m(k+1)}R_{m(jj)} + Q_{m(k+1)}X_{m(jj)}}\right]$$

$$\delta_{m(k+1)} = \delta_{m(k)} - \tan^{-1}\left[\frac{P_{m(k+1)}X_{m(jj)} - Q_{m(k+1)}R_{m(jj)}}{\left|V_{m(k+1)}\right|^2 + P_{m(k+1)}R_{m(jj)} + Q_{m(k+1)}X_{m(jj)}}\right] \tag{11}$$

$$\left(Q_{\text{Loss}}\right)_{m(jj)} = X_{m(jj)} \times \left[\frac{P^2_{m(k+1)} + Q^2_{m(k+1)}}{\left|V_{m(k+1)}\right|^2}\right] \tag{12}$$

$$\left(Q_{\text{Loss}}\right)_{m(jj)} = X_{m(jj)} \times \left[\frac{P^2_{m(k+1)} + Q^2_{m(k+1)}}{\left|V_{m(k+1)}\right|^2}\right] \tag{13}$$

The proposed approach for solving power-flow in imbalanced distribution networks is given in Pseudocode 1.

Pseudocode 1. Proposed approach for solving power-flow in imbalanced distribution networks

```
Procedure PowerFlowAlgorithm():
  # Step 1: Initialization
  Initialize Variables()
    # Step 2: Input values
  InputBaseValues()
  InputLineAndLoadData()
    # Step 3: Initialize voltages
  InitializeVoltages()
    # Step 4: Initialize profit and loss
  InitializeProfitAndLoss()
    # Step 5: Iteration Count
  ITC = 1
    # Step 6: Calculate load current
  CalculateLoadCurrents()
    # Step 7: Calculate branch currents
  CalculateBranchCurrents()
    # Step 8: Calculate voltages using Equations 11 and 12
  CalculateVoltages()
    # Step 9: Calculate voltage difference
  CalculateVoltageDifference()
    # Step 10: Determine maximum voltage deviation
  VMAX = CalculateMaxVoltageDeviation()
    # Step 11: Check if VMAX > 0
  If VMAX > 0 Then
    Goto Step14
    # Step 12: Increment Iteration Count
  ITC = ITC + 1
    # Step 13: Check iteration count limit
  If ITC > ITMAX Then
    Goto Step14
    # Step 14: Calculate real and reactive power losses
  CalculatePowerLosses()
    # Step 15: Present solution
  PresentSolution()
  End Procedure
```

2.1 *Methodology*

This section explains the approach used for the proposed study. The PSO, known for its effectiveness in various research and technological domains, is chosen due to its proven performance and the significance of optimal reconfiguration.

It involves a group of entities (swarms) searching for optimal solutions, resembling food-hunting behavior. Within the search space, particles (solutions) adjust their velocities to find the best solution. Each particle's motion is influenced by its neighbors, collectively aiming for the best global solution. Compared to GA with high mutation rates, crossover effects, computational demands, and complex code, PSO is preferred as a first-choice swarm-based method.

2.2.1 *Implementation of PSO algorithm*

A flowchart for the PSO algorithm implementation is shown in Figure 2. The process starts by assigning a unique bus number to each particle, denoted as $X(1, i)$, chosen randomly within the range of n tie to n bus (as described in equation 4.2). Subsequently, the second step involves initializing the maximum (w_{max}) and minimum (w_{min}) values. Moving to step 3, particle-specific losses are calculated through load flow analysis in each epoch. Step 4 entails searching for optimization opportunities to minimize waste during production. In step 5, particles are adjusted using a given equation. The sixth step sets boundaries for position updates, defining the minimum and maximum. Lastly, in step 7, the entire process is repeated for the next generation, and the cycle continues iteratively.

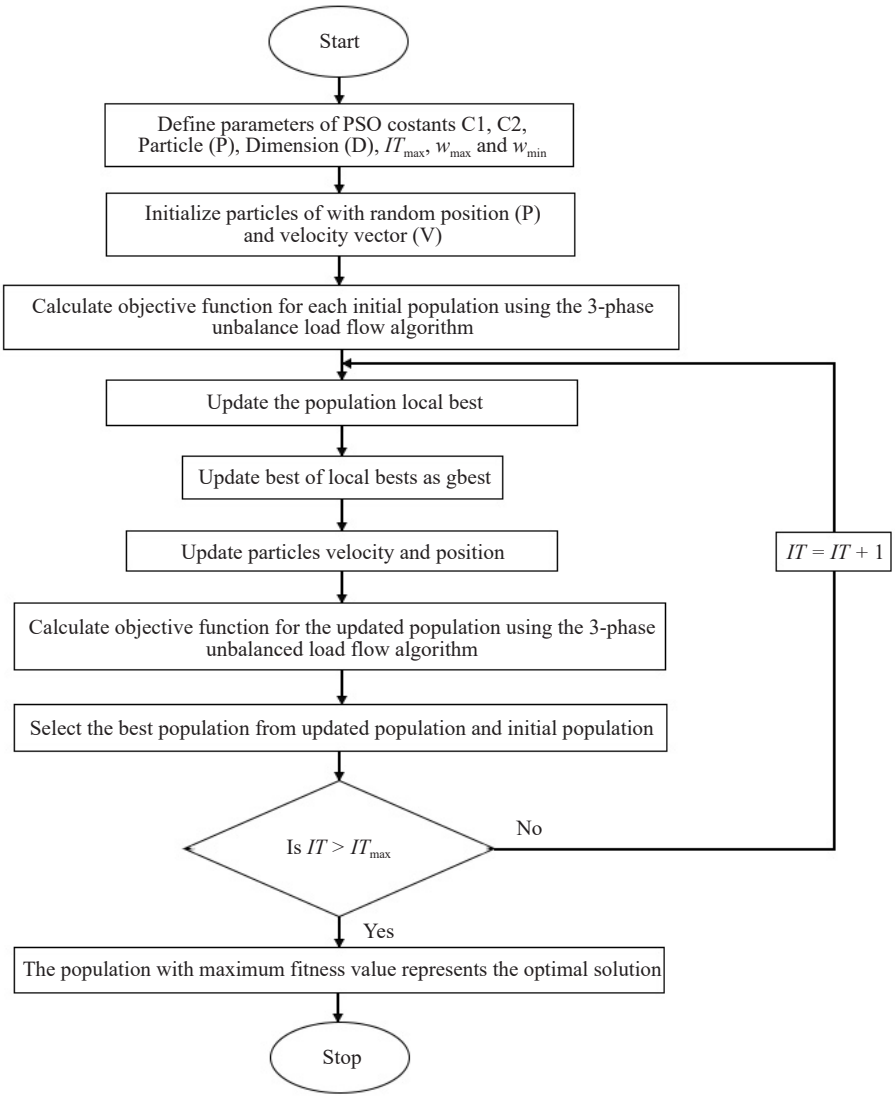

Figure 2. Flow chart of PSO algorithm

2.2.2 *Proposed approach for incorporation of DG model in distribution load flow*

This section delves into the integration of DGs within imbalanced distribution networks. As illustrated in Figure 3, is a segment of an imbalanced distribution system's sample line, accompanied by a connection layout detailing the attachment of three DGs with varying kilowatt (kW) ratings to bus j. Within this context, the different phases-namely, phases a, b, and c-possess their distinct impedances represented as Zijaa, Zijbb, and Zijcc, while phases b, c, and a are characterized by their own impedances, designated as Zijab, Zijcc, and Zijca. It's worth noting that the DG ratings are regarded as constants. When incorporating the DG model, the active power demand at the specific bus housing the DG unit, denoted as bus i, necessitates adjustment to accommodate the DG's influence. The notation Zijaa, Zijbb, and Zijcc denote the self-impedance associated with phase a, phase b, and phase c, respectively. On the other hand, Zijab, Zijbc, and Zijca signify the mutual impedance existing between these different phases. Notably, the DG ratings are treated as continuous values. To incorporate the DG model successfully, a modification is applied to the active power demand at the designated bus, in this case, bus i. This adjustment is captured by equation (14).

$$P_{Dip}^{DG} = P_{Dip}^{base} - P_{ip}^{DG} \tag{14}$$

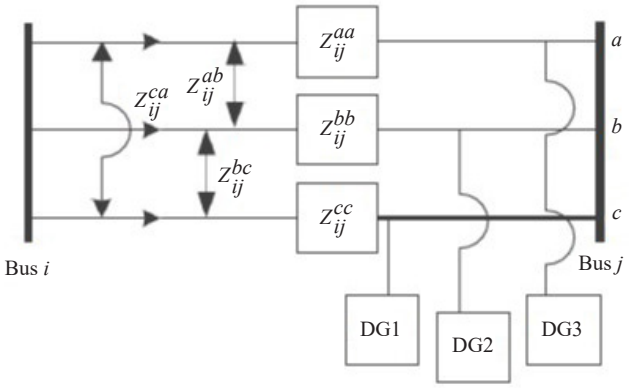

Figure 3. Connection diagram of DGs in a sample unbalanced distribution system

3. Results and discussions

In the section, the proposed PSO solution is applied to the specific radial network while considering its imbalanced load conditions. The suggested methodology is employed to compute the solution. To illustrate the efficacy of this approach, two instances are examined: an unbalanced radial distribution system comprising 19 nodes and an unbalanced radial distribution network encompassing 25 nodes.

3.1 *A 19-node system with and without DG*

Figure 4 is introduced as a visual representation of the 19-node system, as detailed in [28]. To facilitate the efficient transmission of electricity, the base voltage is established at 11,000 V, and the base kVA is set to 103 kVA. Within this framework, the real power consumption is found to be 13.7709 kW, while the reactive power consumption amounts to 5.7956 kVAr. Upon applying the PSO technique, the system is evaluated both with and without DG. The results show that with DG, the real power consumption shifts to 11.497 kW, and the reactive power consumption becomes 4.9464 kVAr.

Table 1 presents a comprehensive comparison of the voltage magnitudes and phase angles of the 19-bus URDS before and after the reconfiguration of the feeder. Following the incorporation of DG, the rewired network exhibits adjusted minimum voltages for each phase: 0.9516 for phase a, 0.9498 for phase b, and 0.9505 for phase c. These values signify an improvement from the initial levels of 0.9553, 0.9535, and 0.9542 per unit (p.u.), respectively. The results underscore the positive impact of the proposed PSO-based methodology in optimizing the performance of the unbalanced

distribution network in the presence of distributed generation.

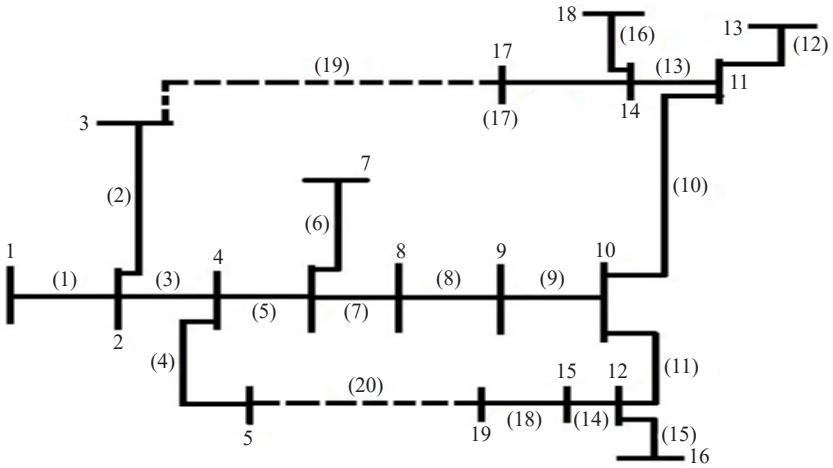

Figure 4. Diagrammatic representation of 19-bus URDN

Table 1. The URDS voltage values of 19-bus without URDN

Bus No.	V(a)	ang (V(a))	V(b)	ang (V(b))	V(c)	ang (V(c))
1.0000	1.0000	0.0000	1.0000	-2.0944	1.0000	2.0944
2.0000	0.9875	0.0003	0.9891	-2.0940	0.9880	2.0953
3.0000	0.9854	0.0000	0.9887	-2.0941	0.9863	2.0958
4.0000	0.9824	0.0006	0.9839	-2.0939	0.9830	2.0955
5.0000	0.9820	0.0006	0.9837	-2.0939	0.9828	2.0956
6.0000	0.9793	0.0007	0.9808	-2.0937	0.9801	2.0957
7.0000	0.9786	0.0008	0.9803	-2.0938	0.9796	2.0957
8.0000	0.9728	0.0011	0.9738	-2.0934	0.9735	2.0958
9.0000	0.9659	0.0015	0.9660	-2.0929	0.9657	2.0959
10.0000	0.9563	0.0019	0.9555	-2.0921	0.9550	2.0962
11.0000	0.9550	0.0018	0.9543	-2.0919	0.9533	2.0963
12.0000	0.9548	0.0020	0.9538	-2.0921	0.9536	2.0962
13.0000	0.9544	0.0018	0.9534	-2.0917	0.9521	2.0963
14.0000	0.9545	0.0018	0.9539	-2.0919	0.9528	2.0964
15.0000	0.9527	0.0022	0.9512	-2.0919	0.9513	2.0962
16.0000	0.9534	0.0023	0.9515	-2.0919	0.9522	2.0961
17.0000	0.9537	0.0019	0.9534	-2.0920	0.9523	2.0965
18.0000	0.9538	0.0018	0.9532	-2.0919	0.9521	2.0964
19.0000	0.9516	0.0024	0.9498	-2.0919	0.9505	2.0962

Table 2. A 19-bus URDS voltage values with DG

Bus No.	V(a)	ang (V(a))	V(b)	ang (V(b))	V(c)	ang (V(c))
1.0000	1.0000	0.0000	1.0000	-2.0944	1.0000	2.0944
2.0000	0.9882	0.0006	0.9898	-2.0938	0.9887	2.0956
3.0000	0.9861	0.0003	0.9894	-2.0938	0.9870	2.0961
4.0000	0.9834	0.0010	0.9850	-2.0934	0.9841	2.0960
5.0000	0.9831	0.0010	0.9847	-2.0935	0.9839	2.0960
6.0000	0.9806	0.0013	0.9821	-2.0932	0.9813	2.0962
7.0000	0.9799	0.0013	0.9816	-2.0933	0.9809	2.0962
8.0000	0.9747	0.0019	0.9757	-2.0927	0.9754	2.0966
9.0000	0.9685	0.0025	0.9686	-2.0918	0.9683	2.0970
10.0000	0.9600	0.0034	0.9592	-2.0906	0.9588	2.0978
11.0000	0.9591	0.0035	0.9584	-2.0903	0.9574	2.0980
12.0000	0.9585	0.0036	0.9575	-2.0905	0.9573	2.0978
13.0000	0.9585	0.0035	0.9575	-2.0901	0.9562	2.0980
14.0000	0.9588	0.0036	0.9582	-2.0901	0.9572	2.0987
15.0000	0.9565	0.0037	0.9550	-2.0903	0.9550	2.0977
16.0000	0.9571	0.0039	0.9552	-2.0904	0.9559	2.0976
17.0000	0.9580	0.0037	0.9577	-2.0902	0.9567	2.0983
18.0000	0.9581	0.0036	0.9575	-2.0901	0.9564	2.0982
19.0000	0.9553	0.0040	0.9535	-2.0904	0.9542	2.0977

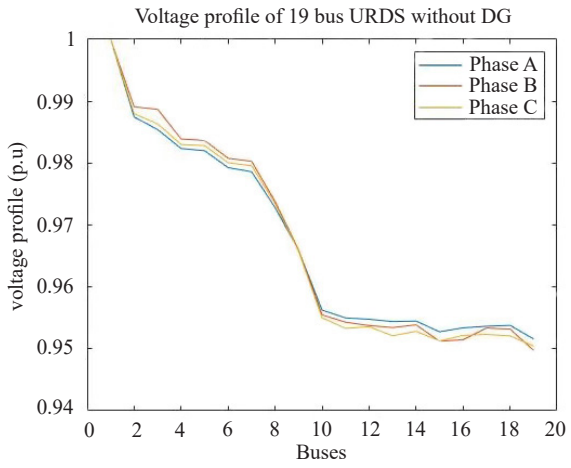

Figure 5. 19-node without DG

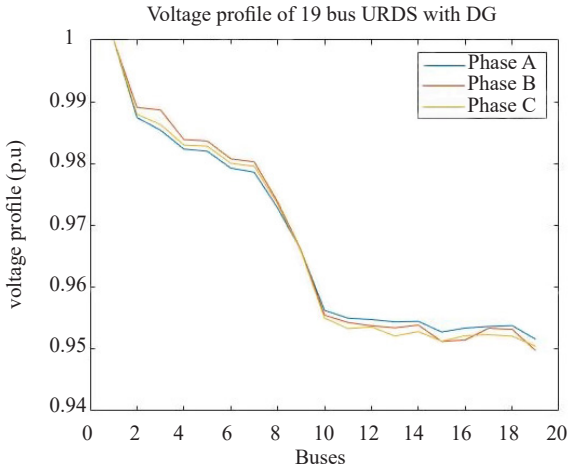

Figure 6. 19-node URDS voltage profile with DG

Table 3. Summary of 19-bus URDS with and without DG

Parameters	Without DG			With DG		
	Phase a	Phase b	Phase c	Phase a	Phase b	Phase c
P_{Total} (kW)	4.4539	4.4533	4.5637	3.8072	3.7964	3.8934
Q_{Total} (kVAr)	1.9405	1.8964	1.9587	1.6587	1.6176	1.6701
V_{mini} (p.u)	0.9516	0.9498	0.9505	0.9553	0.9535	0.9542

Table 2 delves into the voltage magnitude and phase angles of the 19-bus URDS, encompassing the presence of DG. Figure 5 and Figure 6 illustrate the magnitude and direction of voltage changes, as well as power flow across all phases, considering both scenarios with and without DG integration for the 19-node URDN, respectively. Upon the inclusion of DG, the voltage profile undergoes enhancement, while actual power losses are minimized. Table 3 provides a summary of the 19-node URDS, comparing the outcomes with and without DG integration using the PSO technique.

3.2 *A 25-node system with and without DG*

The 25-bus URDS, operating at 4.16 kV, is detailed in reference [33] and visualized in Figure 7. To conduct load flow analysis, an initial voltage of 4,160 V is established, with a chosen base kVA of 103 kVA serving as the reference. Power flow dynamics within this intricate system are visually represented in Figure 8. Furthermore, Figure 12 offers insight into a separate instance of a 25-bus, 4.16 kV URDS. Notably, switches denoted as S25, S26, and S27 are classified as normally open (NO) switches. The power losses, encompassing both real and reactive power are meticulously quantified. In the base scenario, these losses aggregate to 149.9304 kW and 166.9454 kVAr. Upon incorporating the PSO methodology, these values transition to 122.3192 kW and 128.9192 kVAr, irrespective of whether DG is introduced or absent. These findings underscore the effectiveness of the proposed approach in optimizing power loss mitigation within the distribution system. Table 4 shows the repository of information captures alterations in voltage magnitude and phase angles following the feeder's rewiring, specifically excluding DG integration. A closer examination reveals that the rewired network now boasts minimum voltages of 0.9284 for phase a, 0.9285 for phase b, and 0.9366 for phase c. These values contrast with the earlier levels of 0.9325, 0.9329, and 0.9394 p.u., respectively, achieved when DG is introduced. This detailed exploration showcases the substantial impact of the proposed method on system performance, voltage profiles, and power losses.

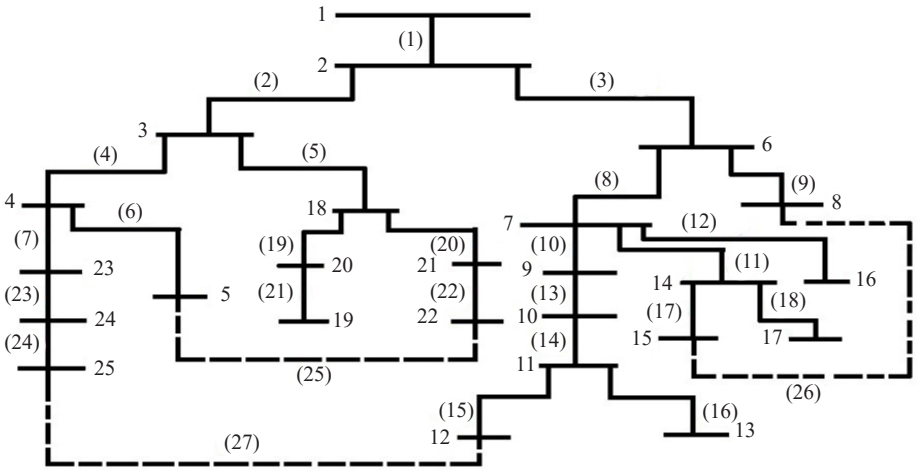

Figure 7. A 25-node URDS

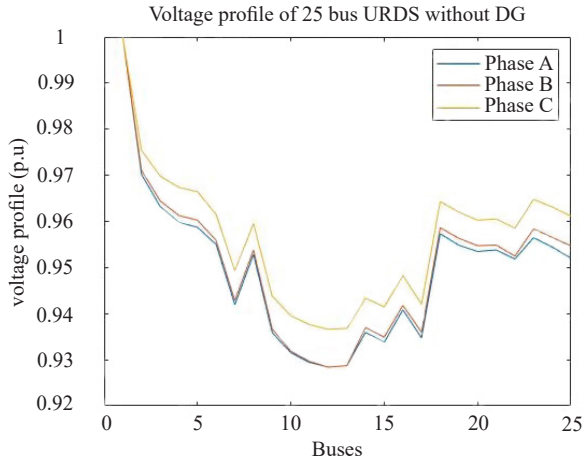

Figure 8. A 25-node URDS voltage profile without DG

Table 5 delves into the voltage magnitude and phase angles of the 25-bus URDS, encompassing the presence of DG. Figures 8 and 9 illustrate the magnitude and direction of voltage changes, as well as power flow across all phases, considering both scenarios with and without DG integration for the 25-node URDN, respectively. Upon introducing DG, the voltage profile undergoes enhancement, while actual power losses are minimized. Table 6 provides a comprehensive summary of the 25-node URDS, comparing outcomes with and without DG integration using the PSO technique. Additionally, Table 7 offers insights into the computational performance of the suggested technique in terms of CPU time and iteration number, in comparison to method [22]. This multi-faceted analysis offers a holistic understanding of the effects of DG integration, the proposed methodology's efficiency, and its comparison with existing approaches.

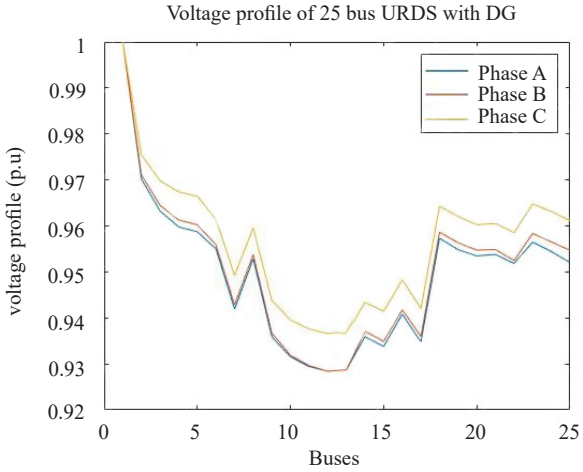

Figure 9. A 25-node URDS voltage profile with DG

Table 4. A 25-bus URDS voltage values without DG

Bus No.	V(a)	ang(V(a))	V(b)	ang(V(b))	V(c)	ang(V(c))
1.0000	1.0000	0.0000	1.0000	-2.0944	1.0000	2.0944
2.0000	0.9702	-0.0099	0.9711	-2.1016	0.9755	2.0824
3.0000	0.9632	-0.0122	0.9644	-2.1034	0.9698	2.0796
4.0000	0.9598	-0.0134	0.9613	-2.1043	0.9674	2.0783
5.0000	0.9587	-0.0133	0.9603	-2.1043	0.9664	2.0783
6.0000	0.9550	-0.0097	0.9559	-2.1006	0.9615	2.0820
7.0000	0.9419	-0.0097	0.9428	-2.0997	0.9492	2.0816
8.0000	0.9529	-0.0097	0.9538	-2.1005	0.9596	2.0820
9.0000	0.9359	-0.0097	0.9367	-2.0993	0.9438	2.0815
10.0000	0.9315	-0.0097	0.9319	-2.0990	0.9395	2.0813
11.0000	0.9294	-0.0097	0.9296	-2.0989	0.9376	2.0813
12.0000	0.9284	-0.0097	0.9284	-2.0988	0.9366	2.0814
13.0000	0.9287	-0.0097	0.9287	-2.0989	0.9368	2.0814
14.0000	0.9359	-0.0096	0.9370	-2.0992	0.9434	2.0814
15.0000	0.9338	-0.0096	0.9349	-2.0990	0.9414	2.0814
16.0000	0.9408	-0.0097	0.9418	-2.0996	0.9483	2.0816
17.0000	0.9347	-0.0096	0.9360	-2.0991	0.9420	2.0815
18.0000	0.9573	-0.0122	0.9586	-2.1030	0.9643	2.0795
19.0000	0.9548	-0.0122	0.9563	-2.1029	0.9620	2.0795
20.0000	0.9535	-0.0122	0.9547	-2.1028	0.9603	2.0795
21.0000	0.9538	-0.0121	0.9549	-2.1029	0.9605	2.0797
22.0000	0.9518	-0.0121	0.9525	-2.1028	0.9585	2.0799
23.0000	0.9565	-0.0133	0.9584	-2.1043	0.9648	2.0783
24.0000	0.9544	-0.0133	0.9565	-2.1043	0.9631	2.0782
25.0000	0.9520	-0.0132	0.9547	-2.1044	0.9612	2.0783

Table 5. A 25-bus URDS voltage values with DG

Bus No.	V(a)	ang(V(a))	V(b)	ang(V(b))	V(c)	ang(V(c))
1.0000	1.0000	0.0000	1.0000	-2.0944	1.0000	2.0944
2.0000	0.9741	-0.0046	0.9751	-2.0970	0.9781	2.0873
3.0000	0.9690	-0.0043	0.9704	-2.0964	0.9738	2.0870
4.0000	0.9656	-0.0054	0.9673	-2.0973	0.9714	2.0858
5.0000	0.9645	-0.0054	0.9662	-2.0972	0.9704	2.0857
6.0000	0.9590	-0.0045	0.9599	-2.0960	0.9642	2.0869
7.0000	0.9459	-0.0044	0.9469	-2.0950	0.9520	2.0865
8.0000	0.9568	-0.0045	0.9579	-2.0958	0.9623	2.0869
9.0000	0.9399	-0.0044	0.9408	-2.0946	0.9466	2.0864
10.0000	0.9356	-0.0044	0.9360	-2.0944	0.9423	2.0862
11.0000	0.9335	-0.0044	0.9338	-2.0943	0.9404	2.0862
12.0000	0.9325	-0.0044	0.9326	-2.0942	0.9394	2.0863
13.0000	0.9328	-0.0044	0.9329	-2.0942	0.9396	2.0862
14.0000	0.9400	-0.0044	0.9411	-2.0945	0.9462	2.0863
15.0000	0.9378	-0.0044	0.9390	-2.0944	0.9442	2.0863
16.0000	0.9449	-0.0044	0.9459	-2.0950	0.9510	2.0865
17.0000	0.9388	-0.0044	0.9401	-2.0945	0.9448	2.0864
18.0000	0.9679	-0.0008	0.9694	-2.0928	0.9725	2.0902
19.0000	0.9654	-0.0008	0.9671	-2.0927	0.9702	2.0902
20.0000	0.9641	-0.0007	0.9656	-2.0926	0.9684	2.0902
21.0000	0.9644	-0.0006	0.9657	-2.0926	0.9687	2.0904
22.0000	0.9625	-0.0006	0.9633	-2.0925	0.9667	2.0906
23.0000	0.9623	-0.0054	0.9644	-2.0972	0.9688	2.0857
24.0000	0.9603	-0.0054	0.9625	-2.0973	0.9671	2.0856
25.0000	0.9579	-0.0053	0.9607	-2.0974	0.9652	2.0857

Table 6. Summary of the 25-bus URDS with and without DG

Parameters	Without DG			With DG		
	Phase a	Phase b	Phase c	Phase a	Phase b	Phase c
P_{Total} (kW)	52.7000	55.4102	41.8284	42.6411	44.9182	34.7599
Q_{Total} (kVAr)	58.2048	53.0695	55.6711	44.6648	41.1201	43.1343
V_{mini} (p.u)	0.9284	0.9285	0.9366	0.9325	0.9329	0.9394

Table 7. Comparison of proposed method as compared to [22]

UBDNs	Without DG				With DG			
	CPU Time		Iteration number		CPU Time		Iteration number	
	PSO	Method [22]	PSO	Method [22]	PSO	Method [22]	PSO	Method [22]
19-node	2.632861	3.130	3	6	0.19417	1.1312	3	6
25-node	1.1730	2.180	5	7	0.146627	0.996	5	7

4. Conclusions

This study introduces a comprehensive framework for modeling components within an imbalanced radial distribution system based on fundamental network theory. Coupled with an efficient power flow technique, this methodology contributes to system solution. By only requiring the identification of buses and branches beyond a single bus once, the algorithm optimizes efficiency. The algorithm's reliable performance is evident through its current summation method, ensuring dependable outcomes. The proposed approach exhibits robust convergence characteristics, particularly in realistic URDS with varying R/X ratios. Comparative analysis against the existing methods, it reveals the superiority of the proposed PSO load-flow analysis for URDNs. Essential factors, including evaluating objective functions, constraint verification through power-flow computation, and accounting for active losses, contribute to the overall calculation time and feasible solution determination. Notably, the method's effectiveness thrives even without requiring optimal power flow, as a higher voltage profile feeder might obviate the need for sectionalizing switch operations, further reducing processing time. Demonstrations using two asymmetric radial distribution test systems underscore its efficacy. Practicing engineers stand to benefit from its expedited comprehension and reduced switching operation demands compared to existing approaches.

5. Future scope

• Expanding the analysis to include multiple conflicting objectives, such as minimizing losses while improving voltage stability.

• Can explore advanced techniques like machine learning algorithms or hybrid optimization methods for an enhance convergence speed and solution accuracy.

• Incorporating renewable energy sources, such as solar and wind, into the imbalanced distribution system could present an interesting extension.

Conflict of interest

There is no conflict of interest for this study.

References

[1] Krishna VM, Sandeep V, Murthy SS, Yadlapati K. Experimental investigation on performance comparison of self excited induction generator and permanent magnet synchronous generator for small scale renewable energy applications. *Renewable Energy*. 2022; 195: 431-441. Available from: https://doi.org/10.1016/j.renene.2022.06.051.

[2] Krishna BM, Sandeep V. An analytical study on electric generators and load control schemes for small hydro isolated systems. In: Vadhera S, Umre BS, Kalam A. (eds.) *Latest Trends in Renewable Energy Technologies. Lecture Notes in*

Electrical Engineering, vol 760. Singapore: Springer; 2021. p.103-119. Available from: https://doi.org/10.1007/978-981-16-1186-5_9.
[3] Pidikiti T, Gireesha B, Subbarao M, Krishna VM. Design and control of Takagi-Sugeno-Kang fuzzy based inverter for power quality improvement in grid-tied PV systems. *Measurement*: *Sensors*. 2023; 25: 100638. Available from: https://doi.org/10.1016/j.measen.2022.100638.
[4] Donta PK, Srirama SN, Amgoth T, Annavarapu CS. Survey on recent advances in IoT application layer protocols and machine learning scope for research directions. *Digital Communications and Networks*. 2022; 8(5): 727-744. Available from: https://doi.org/10.1016/j.dcan.2021.10.004.
[5] Eid A. Allocation of distributed generations in radial distribution systems using adaptive PSO and modified GSA multi-objective optimizations. *Alexandria Engineering Journal*. 2020; 59(6): 4771-4786. Available from: https://doi.org/10.1016/j.aej.2020.08.042.
[6] Stephen HA. *Electric power distribution system engineering*. Estados Unidos; 1986. p.18.
[7] Kersting WH. Distribution system modeling and analysis. In: Grigsby LL. (ed.) *Electric power generation, transmission, and distribution*. 3rd ed. Boca Raton: CRC Press; 2018. p.26.
[8] Ghasemi S. Balanced and unbalanced distribution networks reconfiguration considering reliability indices. *Ain Shams Engineering Journal*. 2018; 9(4): 1567-1579. Available from: https://doi.org/10.1016/j.asej.2016.11.010.
[9] Battula AR, Vuddanti S. Optimal reconfiguration of balanced and unbalanced distribution systems using firefly algorithm. *International Journal of Emerging Electric Power Systems*. 2021; 23(3): 317-328. Available from: https://doi.org/10.1515/ijeeps-2021-0093.
[10] Willis HL. *Power distribution planning reference book*. Boca Raton: CRC Press; 1997.
[11] Miu KN, Chiang HD. Existence, uniqueness, and monotonic properties of the feasible power flow solution for radial three-phase distribution networks. *IEEE Transactions on Circuits and Systems I: Fundamental Theory and Applications*. 2000; 47(10): 1502-1514. Available from: https://doi.org/10.1109/81.886980.
[12] Teng JH, Chang CY. A novel and fast three-phase load flow for unbalanced radial distribution systems. *IEEE Transactions on Power Systems*. 2002; 17(4): 1238-1244. Available from: https://doi.org/10.1109/TPWRS.2002.805012.
[13] Ciric RM, Feltrin AP, Ochoa LF. Power flow in four-wire distribution networks-general approach. *IEEE Transactions on Power Systems*. 2003; 18(4): 1283-1290. Available from: https://doi.org/10.1109/TPWRS.2003.818597.
[14] Ramos ER, Expósito AG, Cordero GÁ. Quasi-coupled three-phase radial load flow. *IEEE Transactions on Power Systems*. 2004; 19(2): 776-781. Available from: https://doi.org/10.1109/TPWRS.2003.821624.
[15] Ranjan R, Venkatesh B, Chaturvedi A, Das D. Power flow solution of three-phase unbalanced radial distribution network. *Electric Power Components and Systems*. 2004; 32(4): 421-433. Available from: https://doi.org/10.1080/15325000490217452.
[16] Wang Z, Chen F, Li J. Implementing transformer nodal admittance matrices into backward/forward sweep-based power flow analysis for unbalanced radial distribution systems. *IEEE Transactions on Power Systems*. 2004; 19(4): 1831-1836. Available from: https://doi.org/10.1109/TPWRS.2004.835659.
[17] Khodr HM, Ocque L, Yusta JM, Rosa MA. New load flow method S-E oriented for large radial distribution networks. In: *2006 IEEE/PES Transmission & Distribution Conference and Exposition*. Latin America. Caracas, Venezuela: IEEE; 2006. p.1-6. Available from: https://doi.org/10.1109/TDCLA.2006.311490.
[18] Abdel-Akher M, Nor KM, Abdul-Rashid AH. Development of unbalanced three-phase distribution power flow analysis using sequence and phase components. In: *2008 12th International Middle-East Power System Conference*. Aswan, Egypt: IEEE; 2008. p.406-411. Available from: https://doi.org/10.1109/MEPCON.2008.4562347.
[19] Penido DR, de Araujo LR, Carneiro S, Pereira JL, Garcia PA. Three-phase power flow based on four-conductor current injection method for unbalanced distribution networks. *IEEE Transactions on Power Systems*. 2008; 23(2): 494-503. Available from: https://doi.org/10.1109/TPWRS.2008.919423.
[20] Kalesar BM, Seifi AR. Fuzzy load flow in balanced and unbalanced radial distribution systems incorporating composite load model. *International Journal of Electrical Power & Energy Systems*. 2010; 32(1): 17-23. Available from: https://doi.org/10.1016/j.ijepes.2009.06.014.
[21] Chen TH, Yang NC. Three-phase power-flow by direct ZBR method for unbalanced radial distribution systems. *IET Generation, Transmission & Distribution*. 2009; 3(10): 903-910. Available from: https://doi.org/10.1049/iet-gtd.2008.0616.
[22] Chen TH, Yang NC. Loop frame of reference based three-phase power flow for unbalanced radial distribution systems. *Electric Power Systems Research*. 2010; 80(7): 799-806. Available from: https://doi.org/10.1016/j.epsr.2009.12.006.
[23] Rafi V, Dhal PK. Maximization savings in distribution networks with optimal location of type-I distributed generator

along with reconfiguration using PSO-DA optimization techniques. *Materials Today: Proceedings*. 2020; 33: 4094-4100. Available from: https://doi.org/10.1016/j.matpr.2020.06.547.

[24] Rafi V, Dhal PK. Loss minimization by reconfiguration along with distributed generator placement at radial distribution system with hybrid optimization techniques. *Technology and Economics of Smart Grids and Sustainable Energy*. 2020; 5: 18. Available from: https://doi.org/10.1007/s40866-020-00088-2.

[25] Atanasovski M, Taleski R. Power summation method for loss allocation in radial distribution networks with DG. *IEEE Transactions on Power Systems*. 2011; 26(4): 2491-2499. Available from: https://doi.org/10.1109/TPWRS.2011.2153216.

[26] Jagtap KM, Khatod DK. Loss allocation in radial distribution networks with various distributed generation and load models. *Electrical Power and Energy Systems*. 2016; 75: 173-186. Available from: https://doi.org/10.1016/j.ijepes.2015.07.042.

[27] Sharma S, Abhyankar AR. Loss allocation for weakly meshed distribution system using analytical formulation of Shapley value. *IEEE Transactions on Power Systems*. 2016; 32(2): 1369-1377. Available from: https://doi.org/10.1109/TPWRS.2016.2571980.

[28] Peng Q, Tang Y, Low SH. Feeder reconfiguration in distribution networks based on convex relaxation of OPF. *IEEE Transactions on Power Systems*. 2014; 30(4): 1793-1804. Available from: https://doi.org/10.1109/TPWRS.2014.2356513.

[29] Taher SA, Karimi MH. Optimal reconfiguration and DG allocation in balanced and unbalanced distribution systems. *Ain Shams Engineering Journal*. 2014; 5(3): 735-749. Available from: https://doi.org/10.1016/j.asej.2014.03.009.

[30] Mirhoseini SH, Hosseini SM, Ghanbari M, Ahmadi M. A new improved adaptive imperialist competitive algorithm to solve the reconfiguration problem of distribution systems for loss reduction and voltage profile improvement. *International Journal of Electrical Power & Energy Systems*. 2014; 55: 128-143. Available from: https://doi.org/10.1016/j.ijepes.2013.08.028.

[31] Lantharthong T, Rugthaicharoencheep N. Network reconfiguration for load balancing in distribution system with distributed generation and capacitor placement. *International Journal of Electrical and Computer Engineering*. 2012; 6(4): 409-414. Available from: https://doi.org/10.5281/zenodo.1076546.

[32] Shami TM, El-Saleh AA, Alswaitti M, Al-Tashi Q, Summakieh MA, Mirjalili S. Particle swarm optimization: A comprehensive survey. *IEEE Access*. 2022; 10: 10031-10061. Available from: https://doi.org/10.1109/ACCESS.2022.3142859.

[33] Vulasala G, Sirigiri S, Thiruveedula R. Feeder reconfiguration for loss reduction in unbalanced distribution system using genetic algorithm. *International Journal of Computer and Information Engineering*. 2009; 3(4): 1050-1058. Available from: https://doi.org/10.5281/zenodo.1084678.